

Correction of Systematic Odometry Errors in Mobile Robots

Johann Borenstein and Liqiang Feng, The University of Michigan
E-mail: johannb@umich.edu, Feng@engin.umich.edu

Abstract

This paper describes a practical method for reducing odometry errors caused by kinematic imperfections of a mobile robot. These errors, here referred to as "systematic" errors, stay almost constant over prolonged periods of time. Performing an occasional calibration as described here will increase the robot's odometric accuracy and reduce operation cost because an accurate mobile robot requires fewer absolute positioning updates. Many manufacturers or end-users calibrate their robots — usually in a time-consuming and non-systematic trial and error approach. By contrast, our method is systematic, provides near-optimal results, and can be performed easily and without complicated equipment.

Experimental results are presented that show a consistent improvement of at least one order of magnitude in odometric accuracy (with respect to systematic errors) for a mobile robot calibrated with the procedure described in this paper.

1. Introduction

In most mobile robot applications two basic position-estimation methods are employed together: *absolute* and *relative* positioning [Chenavier and Crowley, 1992; Evans, 1994]. Relative positioning is usually based on odometry, that is, computing a vehicle's relative motion from the measurement of wheel revolutions and/or steering angles [Everett, 1995]. In most mobile robots, odometry is implemented by means of optical encoders that monitor the wheel revolutions and/or steering angle of the robot's wheels. The encoder data is then used to compute the vehicle's offset from a known starting position. Odometry is simple, inexpensive, and easy to accomplish in real-time. The disadvantage of odometry is its unbounded accumulation of errors.

Because of the accumulation of errors, absolute position corrections are often necessary after as little as 10 m of travel, and they are usually based on external measurements from beacon systems or landmarks (see [Feng et al., 1994] for a detailed discussion of such systems).

These systems require installation and perhaps maintenance, and their cost increases with the number of beacons or landmarks needed. Therefore, improving the odometric accuracy of a mobile robot can dramatically reduce the cost for installation of a mobile robot systems because fewer absolute corrections are required.

2. Properties of Odometry Errors

In a typical *differential drive* mobile robot incremental encoders are mounted onto the two drive motors to count the wheel revolutions. After a short sampling interval I the left and right wheel encoders show a pulse increment of N_L and N_R , respectively. Now, suppose that

$$c_m = \pi D_n / n C_e \quad (1)$$

where

- c_m - Conversion factor that translates encoder pulses into linear wheel displacement.
- D_n - Nominal wheel diameter (in mm).
- C_e - Encoder resolution (in pulses per revolution).
- n - Gear ratio of the reduction gear between the motor and the drive wheel.

One can then compute the incremental travel distance for the left and right wheel, $\Delta U_{L,I}$ and $\Delta U_{R,I}$, according to

$$\Delta U_{L/R,I} = c_m N_{L/R,I} \quad (2)$$

From Eq. (2) it is easy to derive the equations of odometry, which express the horizontal displacement and rotation of the robot (as shown, for example, in [Feng et al., 1994]).

2.1 Systematic and Non-systematic Odometry Errors

Odometry is based on simple equations that are easily implement and that utilize data from inexpensive incremental wheel encoders. However, odometry is based on the assumption that wheel revolutions can be translated into

linear displacement relative to the floor. This assumption is only of limited validity. One extreme example is wheel slippage: If one wheel was to slip on, say, an oil spill, then the associated encoder would register wheel revolutions even though these revolutions would not correspond to a linear displacement of the wheel.

Besides this extreme case of total slippage, there are several other, more subtle reasons for inaccuracies in the translation of wheel encoder readings into linear motion. All of these error sources fit into one of two categories: (1) systematic errors and (2) non-systematic errors.

Non-systematic errors are those that are not directly caused by the kinematic properties of the vehicle (for example: wheel-slippage or irregularities of the floor). On rough surfaces with significant irregularities, non-systematic errors are likely to be the dominant source of odometry errors. On the other hand, systematic errors are particularly grave, because they accumulate constantly. On most *smooth* indoor surfaces systematic errors contribute much more to odometry errors than non-systematic errors.

In most mobile robots systematic errors can be reduced to some degree by careful mechanical design of the vehicle and by vehicle-specific calibration. In this paper we introduce a new method for finding and implementing such calibration factors.

2.2 Definition of Systematic Odometry Errors

The scientific literature, as well as our own experimental experience, indicate that in differential-drive mobile robots there are two *dominant* systematic error sources: *unequal wheel diameters* and the *uncertainty about the effective wheelbase*. We will denote these errors E_d and E_b , respectively. These errors are vehicle-specific and don't usually change during a run (although different load distributions can change some systematic errors quantitatively). Thus, odometry can be improved generally (and in our experience, significantly) by measuring the individual contribution of these two dominant errors sources, and then counter-acting their effect in software.

It is important to note that E_b has an effect only when turning, while E_d affects only straight line motion, as was shown by Borenstein and Feng [1995b]. E_d and E_b are dimensionless values, expressed as fractions of the nominal value. Specifically, we define

$$E_d = D_R/D_L \quad (3)$$

where D_R and D_L are the *actual* wheel diameters of the right and left wheel, respectively. The *nominal* ratio between the wheel diameters is of course 1. We also define

$$E_b = b_{\text{actual}}/b_{\text{nominal}} \quad (4)$$

where b is the wheelbase of the vehicle.

3. Correction of Systematic Odometry Errors

In this section we describe a method for measuring and correcting systematic odometry errors. This method requires two steps: (1) a set of well defined experimental runs, called *UMBmark*, and (2) analysis of the experimental data by means of a set of equations, developed below.

3.1 The experimental procedure "UMBmark"

The *University of Michigan Benchmark* test for mobile robots (UMBmark) is a set of test runs in which the robot is programmed to traverse the four legs of a 4×4 m square path. The path will return the vehicle to the starting area, but, because of odometry and controller errors, not precisely to the starting position. The experimenter measures the absolute position $(x_{\text{abs}}, y_{\text{abs}})$ of the robot before and after each run, using the fixed walls as a reference. These absolute measurements are then compared to the position and orientation of the vehicle as computed from odometry. The result is a set of *return position errors* caused by odometry and denoted ϵx , ϵy .

$$\begin{aligned} \epsilon x &= x_{\text{abs}} - x_{\text{calc}} \\ \epsilon y &= y_{\text{abs}} - y_{\text{calc}} \end{aligned} \quad (5)$$

where

- $\epsilon x, \epsilon y$, — Position errors due to odometry.
- $x_{\text{abs}}, y_{\text{abs}}$ — Absolute position of the robot.
- $x_{\text{calc}}, y_{\text{calc}}$ — Position of the robot as computed from odometry.

This experiment and the associated measurements are performed five times in clockwise (cw) and five times in counter-clockwise (ccw) direction. The rationale for the UMBmark procedure is explained in detail in [Borenstein and Feng, 1995a].

After performing the UMBmark procedure, the experimenter will have gathered five sets of return position errors $(\epsilon x_i, \epsilon y_i)$ for the cw runs, and five sets $(\epsilon x_i, \epsilon y_i)$ for the ccw runs. If plotted, these data points might look similar to the ones shown in Fig. 1. Note that the return positions are clustered in two distinct areas. Averaging the x and y components according to

$$\begin{aligned} x_{c.g.,cw/ccw} &= \frac{1}{n} \sum_{i=1}^n \epsilon x_{i,cw/ccw} \\ &\text{and} \\ y_{c.g.,cw/ccw} &= \frac{1}{n} \sum_{i=1}^n \epsilon y_{i,cw/ccw} \end{aligned} \quad (6)$$

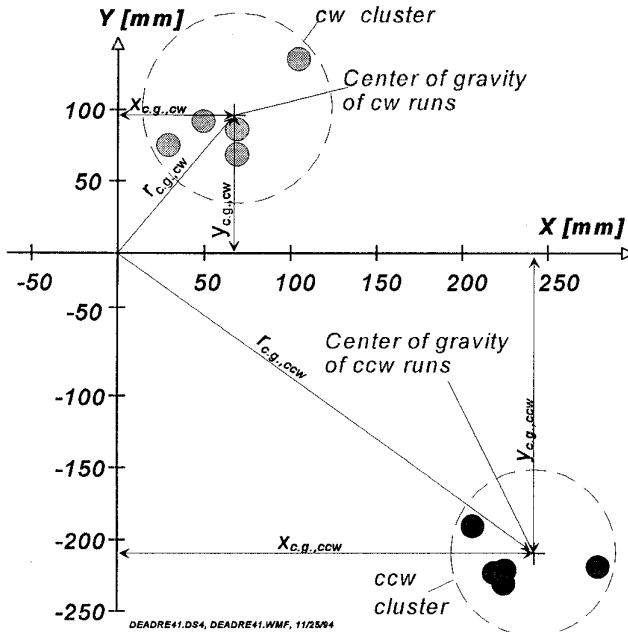


Figure 1: Typical results from running UMBmark (a square path run in both cw and ccw directions) with an uncalibrated vehicle.

yields the center of gravity ($x_{c.g.}$, $y_{c.g.}$) of both the cw and the ccw cluster. Averaging reduces the random effect of non-systematic errors, which cause the spread of the return position errors within each cluster.

3.2 The analytical procedure

One interesting aspect of the error distribution pattern in the UMBmark experiment (see Fig. 1) is the fact that one can analytically derive correction factors from the experimental results. Before we do so, let us first define two new error characteristics that are meaningful only in the context of the UMBmark test. These characteristics, called Type A and Type B, represent odometry errors in orientation. Type A is defined as an orientation error that **reduces (or increases)** the total amount of rotation of the robot during the square path experiment in **both cw and ccw direction**. By contrast, Type B is defined as an orientation error that **reduces (or increases)** the total amount of rotation of the robot during the square path experiment in **one direction**, but **increases (or reduces)** the amount of rotation when going in the **other direction**. Examples are shown in Fig. 2. Figure 2a shows a case where the robot turned four times for a nominal amount of 90° per turn. However, because the actual wheelbase of the vehicle was larger than the nominal value, the vehicle actually turned only 85° in each corner of the square path. In the example of Fig. 2 the robot will actually turn only

$\theta_{total} = 4 \times 85^\circ = 340^\circ$, instead of the desired $\theta_{nominal} = 360^\circ$. We observe that in **both the cw and the ccw** experiment the robot ends up turning **less** than the desired amount, i.e.,

$|\theta_{total, cw}| < |\theta_{nominal}|$ **and** $|\theta_{total, ccw}| < |\theta_{nominal}|$. Thus, the orientation error is of Type A.

In Fig. 2b the trajectory of a robot with unequal wheel diameters is shown. This error expresses itself in a curved path that adds to the overall orientation at the end of the run in ccw direction, but it reduces the overall rotation in the cw direction, i.e.,

$|\theta_{total, ccw}| > |\theta_{nominal}|$ **but** $|\theta_{total, cw}| < |\theta_{nominal}|$. Thus, the orientation error in Fig. 2b is of Type B.

In an actual run Type A and Type B errors will of course occur together. The problem is therefore how to distinguish between Type A and Type B errors, and how to compute correction factors for these errors from the measured final position errors of the robot in the UMBmark test.

3.3 Analysis of Type A and Type B errors

Figure 2a shows the contribution of Type A errors.

We recall our assumption that Type A errors are caused mostly by E_b . We also recall that Type A errors cause too much or too little turning at the corners of the square path. The (unknown) amount of erroneous rotation in each nominal 90° turn is denoted as α and measured in [rad].

Figure 2b shows the contribution of Type B errors. We recall our assumption that Type B errors are caused mostly

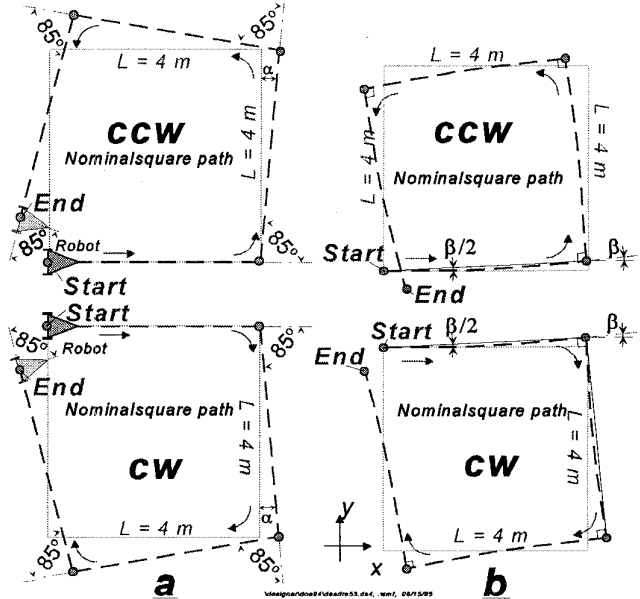


Figure 2: Type A and Type B errors in ccw and cw direction. (a) Type A errors are caused only by the wheelbase error E_b . (b) Type B errors are caused only by unequal wheel diameters (E_d).

by the ratio between wheel diameters, E_d . We also recall that Type B errors cause a slightly curved path instead of a straight one during the four straight legs of the square path. Because of the curved motion, the robot will have gained an incremental orientation error, denoted β , at the end of each straight leg.

We omit here the derivation of expressions for α and β , which can be found from simple geometric relations in Fig. 2 (see [Borenstein and Feng, 1995b] for a detailed derivation). Here we just present the results:

$$\alpha = \frac{x_{c.g.,cw} + x_{c.g.,ccw}}{-4L} \frac{(180^\circ)}{\pi} \quad (7)$$

solves for α in [degrees], and

$$\beta = \frac{x_{c.g.,cw} - x_{c.g.,ccw}}{-4L} \frac{(180^\circ)}{\pi} \quad (8)$$

solves for β in [degrees].

Using simple geometric relations, the radius of curvature R of the curved path of Fig. 2b can be found as

$$R = \frac{L/2}{\sin(\beta/2)} \quad (9)$$

Once the radius R is computed, it is easy to determine the ratio between the two wheel diameters that caused the robot to travel on a curved, instead of a straight path

$$E_d = \frac{D_R}{D_L} = \frac{R + b/2}{R - b/2} \quad (10)$$

The ratio of Eq. (10) can be used to *correct* Type B errors as will be explained in Section 3.3.

Similarly we can compute the wheelbase error E_b . Since the wheelbase b is directly proportional to the actual amount of rotation, we can use the proportion:

$$\frac{b_{actual}}{90^\circ} = \frac{b_{nominal}}{90^\circ - \alpha} \quad (11)$$

so that

$$b_{actual} = \frac{90^\circ}{90^\circ - \alpha} b_{nominal} \quad (12)$$

where, per definition of Eq. (4)

$$E_b = \frac{90^\circ}{90^\circ - \alpha} \quad (13)$$

3.3 Compensation for Systematic Odometry Errors

Once we know the quantitative values of E_d and E_b , it is easy to compensate for these errors in software. The

correction for the wheelbase error E_b is trivial: the wheelbase b is redefined in software according to Eq. (12). The correction for the unequal wheel diameters, E_d , is slightly more complex: After performing the UMBmark procedure, we know the *actual* wheel diameter ratio $E_d = D_R/D_L$ from Eq. (10). However, when applying a compensation factor, we must make sure not to change the *average* wheel diameter D_a , since one would then have to recalibrate that parameter. D_a will remain unchanged if we consider it as a constraint

$$D_a = (D_R + D_L)/2 \quad (14)$$

Solving Eqs. (33) and (39) as a set of two linear equations with two unknowns, D_R and D_L , yields

$$D_L = \frac{2}{E_d + 1} D_a \quad (15)$$

and

$$D_R = \frac{2}{(1/E_d) + 1} D_a \quad (16)$$

We can now define the two correction factors

$$c_L = \frac{2}{E_d + 1} \quad (17a)$$

$$c_R = \frac{2}{(1/E_d) + 1} \quad (17b)$$

which can be implemented in the odometry algorithm by rewriting Eq. (2) as

$$\Delta U_{L/R, I} = c_{L/R} c_m N_{L/R, I} \quad (18)$$

We have thus corrected both dominant systematic errors.

4. Experimental Results

In this section we describe experiments that validate the above described method for correcting Type A and Type B errors by changing the effective wheelbase b and the effective wheel-diameter ratio D_R/D_L . The experiments were performed with a TRC *LabMate* robot equipped with an onboard 486/50 MHz PC compatible computer.

To avoid slippage, the robot was traveling slowly, at a speed of 0.2 m/s during the straight legs of the square path. At the end of each leg the robot came to a complete stop and rotated on-the-spot through 90°. This means that the robot made a fourth 90° turn after returning to its starting area.

The difference between the absolute position and the perceived position is called the *return position error* ϵ ; ϵ is defined by Eqs. (5), above.

The uncalibrated robot (i.e., $D_R/D_L = 1.0000$ and $b = b_{\text{nominal}} = 340.00$ mm) made five cw trips and five ccw trips. As expected, the *return position errors* were clearly grouped in a cw cluster and a ccw cluster. For each of the two clusters the x and y components of the respective centers of gravity were computed according to Eq. (5). The resulting $x_{c.g.}$ and $y_{c.g.}$ were used to compute E according to Eqs. (8) - (10). Then, correction factors c_L and c_R were computed according to Eqs. (17) and (18) and introduced into the dead-reckoning program. Similarly the corrected wheelbase b_{new} was computed according to Eqs. (11) - (13) and revised in the robot's odometry program.

At this time the calibration procedure was complete. In order to verify the results we ran the UMBmark experiment for a second time, this time with the correction factors in place. Figure 3 shows the results of both the uncalibrated runs and the runs with the calibrated vehicle.

$$r_{c.g.,cw} = \sqrt{(x_{c.g.,cw})^2 + (y_{c.g.,cw})^2}$$

and

$$r_{c.g.,ccw} = \sqrt{(x_{c.g.,ccw})^2 + (y_{c.g.,ccw})^2}$$

To compare the accuracy of the robot before and after calibration, we examine the absolute offsets of the two centers of gravity from the origin, $r_{c.g.,cw}$ and $r_{c.g.,ccw}$ (see Fig. 1). We define the larger value among $r_{c.g.,cw}$ and $r_{c.g.,ccw}$ as the *measure of dead-reckoning accuracy for systematic errors*

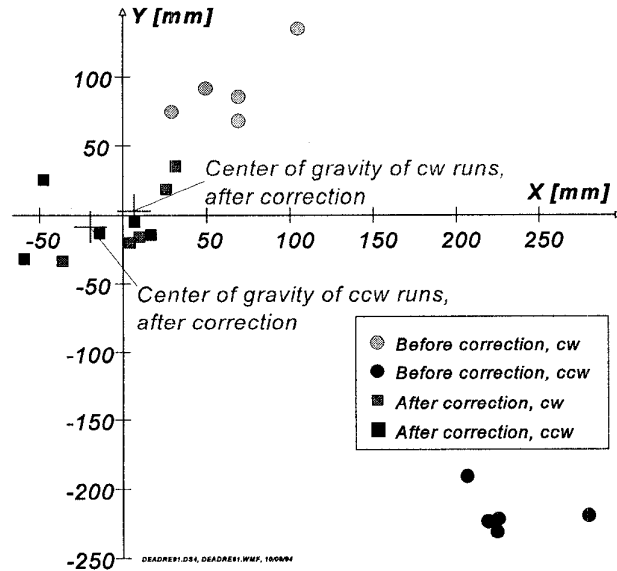


Figure 3: Position Errors after completion of the UMBmark Experiment (4 x 4 m bi-directional path).

Before calibration: $b=340.00$ mm, $D_R/D_L = 1.00000$
After calibration: $b=336.17$ mm, $D_R/D_L = 1.00084$

$$E_{\text{max,syst}} = \max(r_{c.g.,cw} ; r_{c.g.,ccw}) \quad (20)$$

In the example of Fig. 3, $E_{\text{max,syst}}$ was 317 mm before compensation and 21 mm after compensation. This represents a 15-fold improvement.

While developing this method, we performed a total of eight carefully monitored experiments. The results are listed in Table I.

Experiment #	$E_{\text{max,syst}}$ before compensation [mm]	$E_{\text{max,syst}}$ after compensation [mm]	Improvement
1 ⁺	317	21	15-fold
2	349	32	11-fold
3 [†]	310	31	10-fold
4 [†]	310	14	22-fold
5 [†]	310	26	12-fold
6	403	35	11-fold
7*	423	after 1st comp: 66 after 2nd comp: 20	21-fold
8 [‡]	232	12	19-fold

⁺) Details shown in Fig. 7

[†]) These 3 experiments used the same set of uncalibrated results and identical correction factors.

^{*}) In this experiment the diameter of the right wheel was slightly increased by winding three loops of masking tape around the wheel perimeter. Also: two compensation runs were performed. See explanation in main text.

[‡]) In this experiment the diameter of the left wheel was slightly increased by winding five loops of masking tape around the left wheel perimeter.

Table I: Dead-reckoning Accuracy for Systematic Errors, $E_{\text{max,syst}}$ before and after compensation.

The seemingly large fluctuations in improvement, especially among experiments #3, #4, and #5 (which all used the same correction factors) are due to the fact that the *centers of gravity* (c.g.s) for the runs after calibration are all very close to the origin (as seen in Fig. 3). Thus, the arbitrary spread of return position errors caused by non-systematic error sources has greater impact on the c.g.s. For example, the c.g. of Experiment 4 is only 17 mm (5/8") closer to the origin than the c.g. of Experiment #3 — a difference that is easily attributable to the arbitrary spread of non-systematic errors.

In principle, it is possible to achieve even better results by performing the compensation procedure for a second time, "on top of" the first compensation. This is so because a compensated robot can be treated as though it was a

"new" uncompensated robot, but with different initial parameters. Using the *standard deviation* (σ) of the 5 runs in each direction it is easy to decide when a second compensation run will be beneficial. The σ of the *return position errors* in the UMBmark experiment was about 25 mm. The *Standard Error of the Mean* (SEM), defined as $SEM = \sigma/\sqrt{n}$ was 11.2 mm (n is the number of runs). As a rule-of-thumb sometimes used in small sample statistics [Walpole and Myers, 1985], one can say that if $E_{\max, \text{sys}} < 3 \times \text{SEM}$ it is unlikely (here: a likelihood of 5%) that the result can be improved by a second compensation. We put this rule-of-thumb to the test in Experiment #7, where $E_{\max, \text{sys}} = 66$ mm was notably worse (the improvement over the uncompensated run was only 6.4-fold) than in the other experiments. Applying the above rule-of-thumb, it is evident that $66 \text{ mm} > 3 \times \text{SEM} = 33.6 \text{ mm}$, so that a second compensation run was indicated. After the second compensation, the vehicle's error was $E_{\max, \text{sys}} = 20$ mm, i.e., a 21-fold reduction relative to the uncompensated systematic error.

5. Conclusions

This paper presents a method for the correction of systematic odometry errors in differential-drive mobile robots. The paper investigates specifically the errors due to the *wheel diameter ratio*, E_d , and the *uncertainty about the wheelbase*, E_b .

The focus on E_d and E_b is based on our error model, which assumes that systematic orientation errors are either of Type A or Type B. Type A errors are directly affected by E_b and Type B errors are directly affected by E_d . Other systematic errors may also affect the overall Type A and Type B error. However, there is no need to worry about this, because, in principle, both Type A and Type B errors can be eliminated completely by changing the effective wheelbase and wheel-diameter ratio in software.

The main contribution of this paper is the definition of a systematic procedure for correcting Type A and Type B odometry errors. The effectiveness of this procedure and the validity of its underlying model are supported by the experimental results. The results show that by changing only the effective wheelbase and the effective wheel-diameter ratio the vehicle's odometric accuracy (with respect to systematic errors only) increased by at least one order of magnitude. This improvement was consistent when tested repeatedly for the same vehicle and when tested on the same vehicle but with artificially altered wheelbases and wheel-diameter ratios.

One should note that odometric calibration factors are used by many researchers. However, to date such factors were usually found by some form of trial-and-error and some intuition on the part of the experimenter. This type

of approach is very time consuming and yields inferior results. By contrast, the procedure described here offers a systematic approach that yields near-optimal results. The strength of the UMBmark calibration procedure lies in the fact that even minute mechanical inaccuracies, such as wheel diameters that differ by as little as 0.1% can be isolated and identified.

Acknowledgments: This research was funded by NSF grant # DDM-9114394 and by Department of Energy Grant DE-FG02-86NE37969. The authors thank Mr. Brian Costanza and Mr. Brad Holt for conducting many of the experiments.

6. References

1. Borenstein, J. and Feng, L., 1995a, "UMBmark: A Benchmark Test for Measuring Odometry Errors in Mobile Robots." To be presented at the SPIE Conference on Mobile Robots, Philadelphia, Oct. 22-26.
2. Borenstein J. and Feng, L., 1995b, "Measurement and Correction of Systematic Odometry Errors in Mobile Robots." Accepted for publication in the *IEEE Journal of Robotics and Automation*, May 1995.
3. Chenavier, F. and Crowley, J., 1992, "Position Estimation for a Mobile Robot Using Vision and Odometry." *Proceedings of IEEE International Conference on Robotics and Automation*, Nice, France, May 12-14, pp. 2588-2593.
4. Evans, J. M., 1994, "HelpMate: An Autonomous Mobile Robot Courier for Hospitals." *1994 International Conference on Intelligent Robots and Systems*. Munich, Germany, September 12-16, pp. 1695-1700.
5. Everett, H.R., 1995, "Sensors for Mobile Robots," A K Peters, Ltd., Wellesley, MA, publ. date: Fall 1995.
6. Feng, L., Borenstein, J., and Everett, B., 1994, "Where am I? Sensors and Methods for Autonomous Mobile Robot Localization." *Technical Report, The University of Michigan, available via anonymous FTP from ftp.eecs.umich.edu/f/people/johannb*.
7. Walpole, R. E. and Myers, R. H., 1985, "Probability and Statistics for Engineers and Scientists," 3rd edition. Macmillan Publishing Company, New York, New York 10022.